Journal of Archaeological Science: Reports xxx (xxxx) xxx–xxx

Contents lists available at ScienceDirect

Journal of Archaeological Science: Reports

journal homepage: www.elsevier.com/locate/jasrep

Ecosystem modeling using artificial neural networks: An archaeological tool

Lidia Susana Burry[a,*], Bernarda Marconetto[b], Mariano Somoza[a], Patricia Palacio[a,c], Matilde Trivi[d], Hector D'Antoni[e]

[a] Laboratorio de Palinología y Bioantropología, Departamento de Biología, Facultad de Ciencias Exactas y Naturales, Universidad Nacional de Mar del Plata, (UNMdP), Funes 3250, (CP7600) Mar del Plata, Argentina
[b] Instituto de Antropología de Córdoba, (IDACOR), CONICET, FFyH, Universidad Nacional de Córdoba, Av. Hipólito Yrigoyen 174, (CP 5000) Córdoba, Argentina
[c] CONICET, Argentina
[d] Facultad de Psicología, Universidad Atlántida Argentina, Arenales 2740, (CP7600) Mar del Plata, Argentina
[e] NASA Ames Research Center, CA, United States

ARTICLE INFO

Keywords:
Paleo-NDVI
Hindcasting
Artificial Neural Network
Ecosystem modeling
Argentina

ABSTRACT

Prediction of past Normalized Difference Vegetation Index (paleo-NDVI) in Valle de Ambato (Catamarca, Argentina) in the periods of 550–650 and 1550–1650 CE was carried out to test the efficacy of Artificial Neural Network (ANN) to predict past environments for Archaeology. This work shows that both subtropical Yunga and xerophytic Chaqueña vegetations respond in contrasting fashion to changes in climate forcings. To predict the past an ANN perceptron multilayer model was used. Modern NDVI data and Tree-Ring data were obtained from NOAA-Paleoclimate, and other public sources. These data were used to train the model. Real data and predictions were close (Pearson correlation 0.83–0.90) and warranted the following step, hindcasting. Important paleo-NDVI fluctuations lasting 15 to 20 years were identified in both periods under study. The paleo-NDVI fluctuations in the earlier period were probably related to the unidentified eruption of 583. The fluctuations in the later period appear related to the eruption of 1600 of the Huaynaputina volcano (SW Peru). These findings suggest that the model accurately identified vegetation fluctuations in response to changes in the volcanic forcing. Hence, the ANNs may be considered as apt tools for modeling past environments in support of archaeology.

1. Introduction

This paper presents a hindcast of the Normalized Difference Vegetation Index (NDVI) within two periods (550–650 and 1550–1650 CE) of significant ecosystem changes in north of Valle de Catamarca (Catamarca, Argentina).

This index relates the absorbed photosynthetically active radiation (PAR) in the range of 400 to 700 nm used for photosynthesis, and the near infrared, from 700 nm up to 1100 nm, mostly reflected by the foliar structures of plants. The NDVI is a good indicator of various vegetation parameters for it provides a strong vegetation signal and a good spectral contrast of most reference materials (Tucker and Sellers, 1986). Also when training our Neural Net model, we want to have as much of historical information and observed variance as possible. This is why we use AVHRR-NDVI.

Our hindcast was performed on two pixels belonging to the Yunga plant geographical province and on one to the Chaqueña plant geographical province (Cabrera, 1976; Palmieri et al., 2014). These three pixels were selected because they (a) reflect the most contrasting environmental settings north of the Valley and are placed in the Valley's opposite slopes, (b) have the best correlation in the train step of Artificial Neuronal Network (ANN) and, (c) have the largest variability in the Valley during the periods analyzed in this work.

We are interested in further understanding the ecosystem responses on each slope of the Valley to changes in one climate forcing, and offer background to the dynamic of human settlements through time in connection with environmental changes.

The choice of these pixels was based on the relatively low human activity at the present time. Therefore, the modern data collection used to train the ANN model contains data with little human impact. This responds to a general rule in paleobiological research: first reconstruct the environmental history free of human impact in order to offer this reconstruction to comparative analysis when the reconstruction is performed in an area of human activity and hence impact.

There are a few previous works applying this approach to modeling. An ANN predictive model was used to hindcast the Sea Surface

* Corresponding author.
E-mail addresses: lburry@mdp.edu.ar (L.S. Burry), ppalacio@mdp.edu.ar (P. Palacio), mtrivi@mdp.edu.ar (M. Trivi).

http://dx.doi.org/10.1016/j.jasrep.2017.07.013
Received 6 December 2016; Received in revised form 1 July 2017; Accepted 12 July 2017

Temperature (SST) of the Pacific Ocean close to South America and the South Atlantic linking SST to Tree Ring widths over the period of 1246–2000 CE (D'Antoni and Mlinarevic, 2002; D´Antoni, 2008). The correlation of SST with the NDVI of South American plant communities was tested with an ANN predictive model over the period 1982–2000 CE (D'Antoni et al., 2002). Hindcasting of paleo-NDVI on eleven pixels of Valle de Ambato over the period of 442–1998 was carried out using ANN models (Marconetto et al., 2015). Further applications of this method were developed in the progress report to the NASA Astrobiology Institute (D'Antoni et al., 2008).

Other methods have been used for predicting the past, particularly those based on linear regression. These are all good and reliable for interpolation work. However, when hindcasting, the calibration dataset has necessarily a shorter timespan. Hence, a large part of the work is extrapolation where linear prediction is less reliable. Neural Network models using the sigmoid function are equally reliable in prediction and in hindcasting (Adya and Collopy, 1998; Bandyopadhyay and Chattopadhyay, 2007; Cigizoglu, 2003; Russell and Norvig, 2003).

Paruelo and Tomasel (1997) predicted NDVI from time series of temperature and precipitation of the 20th century using regression models and ANN. These authors got better results with ANN because, they submit, ANNs relate temperature and precipitation data of previous years that are connected with ecosystem functioning in the following years.

In this work it was possible to demonstrate the contrasting responses of Yunga and Chaqueña vegetation to the effects of climate forcings north of Valle de Catamarca over the periods of 550–650 and 1550–1650 CE while offering further detail than in previous works (Marconetto et al., 2015).

The understanding of past environmental variations with the aim of assembling them with the dynamics of human occupations implies in turn the comprehension of climate forcings, perhaps linked to the anomalies observed in retrodictive models.

In a previous work (Marconetto et al., 2015) as a result of the ecosystemic model built for 11 pixels covering the northern Valley of Catamarca until 442 CE, two moments were particularly observed that caught our interest. They refer to two situations where the behavior of positive and negative anomalies of NDVI was substantial and complex to be explained. We then hypothetically associated the 20th century observations to global events, e.g. Little Ice Age. Nevertheless, the potential role of volcanic eruptions cannot be discarded. Volcanic eruptions are a dominant driver of naturally forced climate variability during the last millennium (Colose et al., 2016).

In this line it is suggestive the mention and description of the eruption of the Huaynaputina volcano (south of Peru) by the Mercedarian Martín de Murúa, illustrated and mentioned by the chronicler Guamán Poma de Hayala (Fig. 1) (Lavallé, 2011). The episode is narrated by chroniclers as a relevant and significant event, and studies on volcanism mention that the eruption generated recorded global events.

> LA CIVDAD DE ARIQVIPA: Rebentó el bolcán y cubrió de zeníza y arena la ciudad y su juridición, comarca; treynta días no se bido el sol ni luna, estrellas. Con la ayuda de Dios y de la uirgen Santa María sesó, aplacó.
>
> Le fue castigado por Dios cómo rreuentó el bolcán y sallió fuego y se asomó los malos espíritus y salió una llamarada y humo de senisa y arena y cubrió toda la ciudad y su comarca adonde se murieron mucha gente y se perdió todas las uiñas y agiales y sementeras.
>
> Escurició treynta días y treynta noches. Y ubo procición y penetencia y salió la Uirgen María todo cubierto de luto y ancí estancó y fue seruido Dios y su madre la Uirgen María. Aplacó y pareció el sol pero se perdió todas las haziendas de los ualles de Maxi. Con la senisa y pistelencial de ella se murieron bestias y ganados.
>
> *LA VILLA DE ARICA tanbién fue cubierto de seniza del bolcán toda la cordellera de la mar.* (Guamán Poma de Hayala, 1615).

It has been paralleled to the nineteenth century Krakatoa eruption (de Silva and Zielinski, 1998). According to Costa et al., 2003) the eruption of Huaynaputina is an example of the effectiveness of explosive silicic arc magmas at producing short term although abrupt climate changes.

Certainly, global events produce different effects on ecosystems with different limiting factors; however, we find it interesting to explore this variable in relation to our model, particularly because of the proximity at global scale of the Haynaputina volcano with the Argentine northwestern.

2. Materials and methods

2.1. Study area

The study area is the north of Valle de Catamarca, in the surroundings of Valle de Ambato (Catamarca province) (27°48′ to 28°04′S and 65°46′ to 65°56′W) in Northwestern Argentina. The area is orographically heterogeneous; therefore, it also holds diverse plant communities. The valley lies in the Sierras Pampeanas and limits with the summits of Sierra de Humaya to the west and Graciana Balcozna to the east (Fig. 2). Annual precipitation varies from 500 to 800 mm and most of the rain falls in summer. Mean temperature is 25 °C in the warmest month and 9 °C in the coldest (de la Orden and Quiroga, 1997; Palmieri et al., 2005). Elevation and exposure of the slopes give climatic peculiarities to the different sectors. Within this frame, de la Orden and Quiroga (1997) have established different vegetation units (Fig. 3).

On the Eastern and Northeastern sides of the Valley, Eastern slope of the Graciana Balcozna Hills, is the Yunga Plant Geographical Province, with montane forest and grasslands in the hill summits (Morláns, 1995). Elements of this vegetation appear on the western slopes. The climate is warm and humid with abundant rainfall in summer and frost in winter (Cabrera, 1976). The Yunga receives humidity from the low level jet of South America (Insel et al., 2010; Virji, 1981) forming the fog forest (Hunzinger, 1997). Therefore, Yunga gets water from vertical as well as horizontal precipitation. This horizontal precipitation (fog) is the one that crosses through the Graciana Balcozna Hills summits and covers the grassland area of the western side of the hills. Consistently, the east slope side pixels show NDVI annual average larger than 0.60 (Burry et al., 2017) for this environment with no restrictions for humidity.

In contrast, on the west side of the Valley, the vegetation belongs to the Chaqueña Plant Geographical Province (Chaco Serrano District) with warm and drier climate conditions (Cabrera, 1976). The Chaco Serrano covers the summit and the eastern slopes of Sierra de Humaya. Its characteristic vegetation arranges in “belts” or “levels” with particular structure and composition (Morláns, 1995). The presence of xerophytic vegetation (xerophytic forest and patches of grass and shrubs) is related to an annual NDVI average of around 0.5, reflecting an environment with moisture restriction. Also, the annual values of NDVI show a large variation range that underscore the sensitivity of grassland NDVI to the effects of drought (Zerda and Tiedemann, 2010).

Two pixels (2 and 5) belonging to the Yunga, and another one (pixel 6) from the Chaco Serrano District were selected within the study area. Pixel 2 located to the east of Sierra Graziana Balcozna has a montane forest vegetation, while pixel 5, in the eastern and western slopes show forest and grasslands upon the summit. Pixel 6 has mainly shrubby vegetation, dry forest southwest of the pixel, and grasslands upon the summit (FAO, 2014, de la Orden y Quiroga 1997, Morláns, 1995).

2.2. Materials (data)

(a) Satellite: NDVI from the Global Inventory Modeling and Mapping Studies, GIMMS (GLCF, Tucker et al., 2004) derived from satellite images AVHRR with 8 km pixels (AVHRR sensor mounted in NOAA

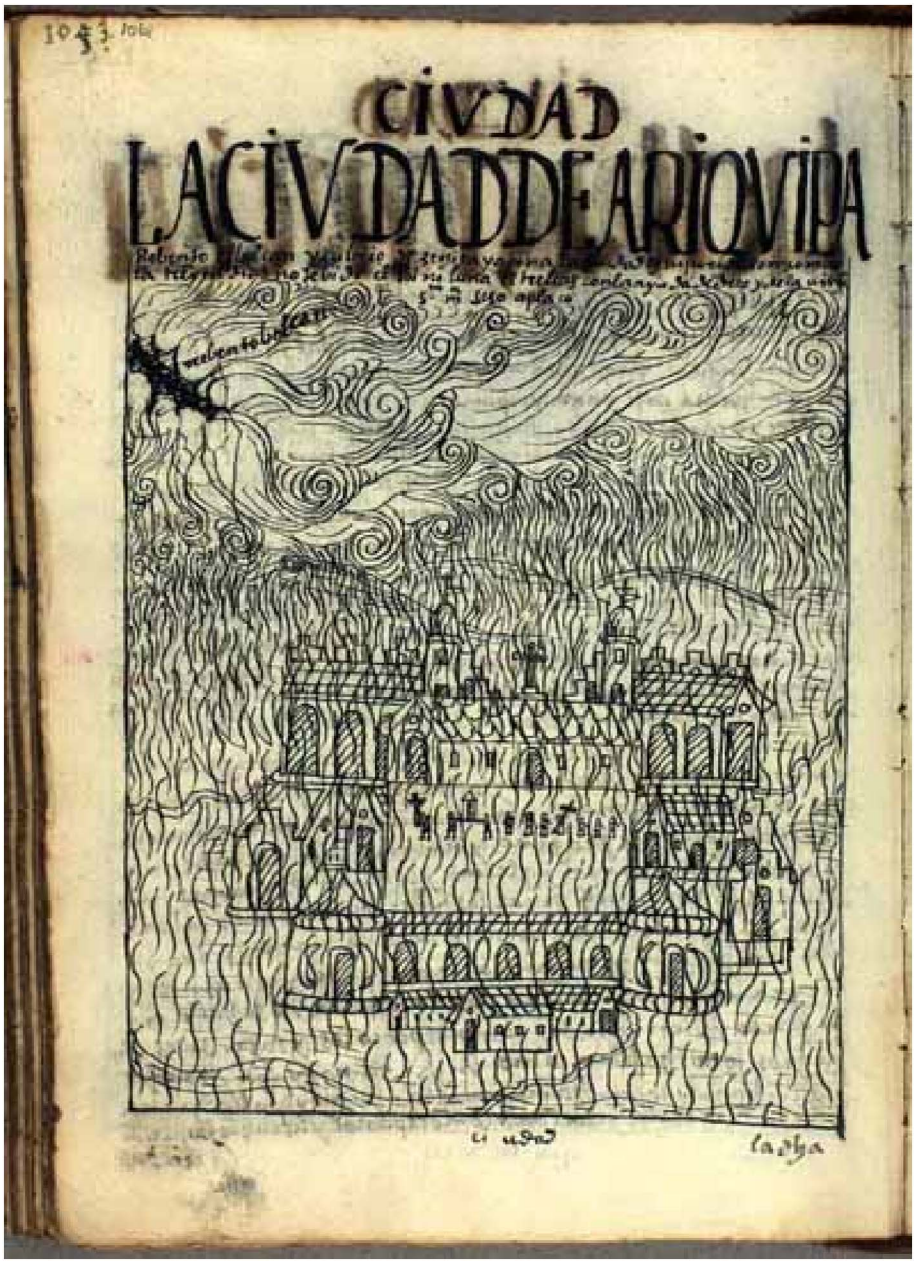

Fig. 1. Epoch engraving of Guamán Poma de Hayala (1615). Arequipa City (Peru) with ashes from the Huaynaputina volcano.

series 7, 9, 11, 14, 16 and 17). GIMMS-NDVI data from database are corrected for radiometric effects before making it available to the users.

(b) Tree-ring widths from International Tree Ring Data Bank and World Data Center (Paleoclimatology archives). Nine chronologies of *Juglans australis* and *Cedrella angustifolia*, from Northwestern Argentina for the period of 1765–1985 CE (Villalba et al., 1985, 1992) (Table 1). These tree rings are out of the study area. Also four chronologies of *Fitzroya cupressoides*, from Patagonia for the period of 342–1995 (Lara et al., 2000; Villalba et al., 1996) (Table 2).

(c) Oxygen and Hydrogen isotopes, atmospheric gasses, non-marine sulfates (Cole-Dai et al., 2000; Jiang et al., 2012; Mosley-Thompson et al., 2003, Zhou et al., 2006; Zielinski et al., 1994) and a cosmogenic, Beryllium 10, (Bard et al., 2007, 2003, 2000, 1997) extracted from Greenland and Antarctica ice cores for the period of 442–1998 CE, World Data Center for Paleoclimatology Archives.

(d) Missing tree ring data in the chronologies of Northwestern Argentina were simulated using ANN trained with the data from ice cores and the tree rings from Patagonian chronologies.

3. Methods

For hindcasting, we have used the "Vegetation History" module of the Hindcasting Ecosystem Model, HEMO, (D'Antoni et al., 2008) and specifically the ANN program included in the WEKA software pack (Hall et al., 2009).

3.1. Artificial Neural Network (ANN)

The ANNs are artificial-intelligence tools that use non-linear functions and operate in analogous manner to that of the nervous system. The ANNs are formed with nodes or neurons of three types: input (data), hidden (processing) and output (results). The nodes tridimensionally integrated form the network. In the data processing a statistical weight is assigned to each node. The ANN is "trained" using real data for the predictors as well as for the variable to be predicted. The training is carried out with examples that repeat what they learned and ends when all those data that were assigned weight were included in the model. After the construction of the training model, comes the

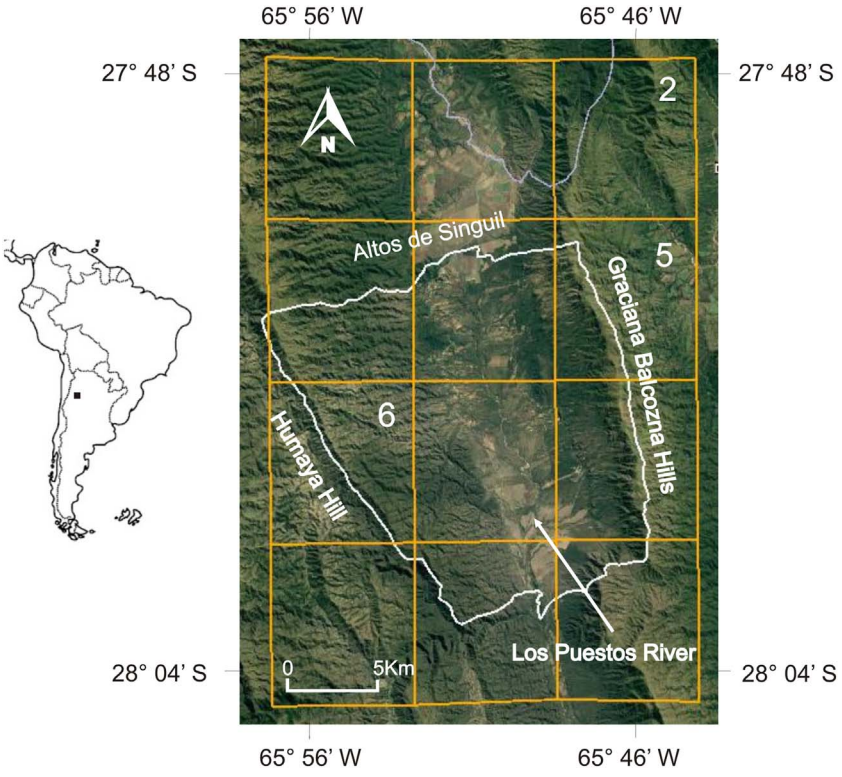

Fig. 2. Location and orography of the study area. In white: Valle de Ambato; 2, 5 and 6: studied pixels.

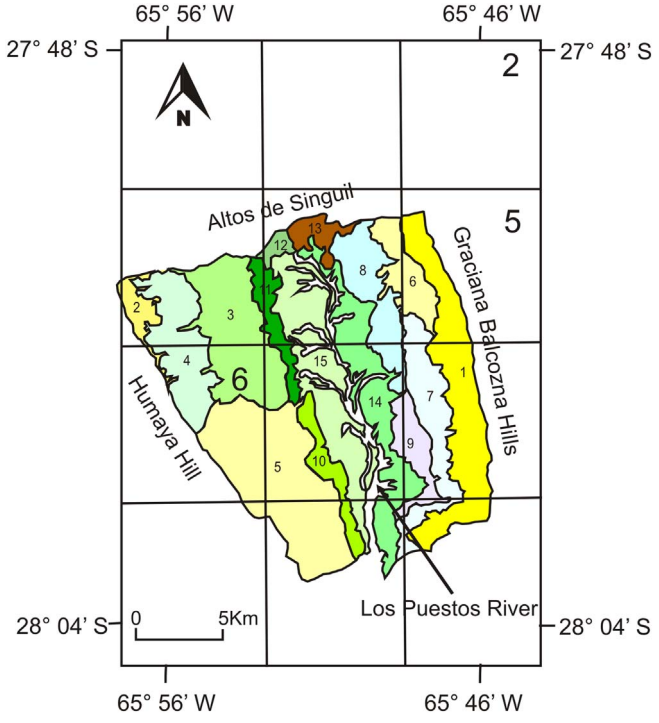

Fig. 3. Vegetation of Valle de Ambato, Catamarca, Argentina (modified from de la Orden and Quiroga, 1997). 1. Grassland (summits of Graziana Balcozna Hill), 2.Grass (summits of Humaya Hill), 3.Grassland-shrubland mosaic, 4. Grassland-suffrutices mosaic, 5. Forest, 6. Grassland (piedmont Graziana Balcozna Hill), 7.Forest-shrubland mosaic (piedmont sup.), 8. Forest-shrubland mosaic (piedmont inf.), 9. Open forest (piedmont), 10. Forest (piedmont Humaya Hill), 11. Grassland-shrub mosaic (piedmont Humaya Hill), 12. Grassland with shrub (Altos de Singuil), 13. Shrubland, 14. Open forest (fluvial plain), 15. Forest gallery (fluvial plain).

validation to ensure that the results are acceptably accurate. Then, the model is ready to make predictions or hindcasts. The learning is a critical step that should be performed with data that contain the largest range of variation in order to produce robust predictions. The perceptron multilayer is a much used algorithm that consists of several single perceptron layers that relate among themselves by means of a back-propagation algorithm (Russell and Norvig, 2003). Back propagation of errors allows a balance of all perceptron weights and establishes non-linear relations (Hall et al., 2009) while building the model. The ANNs are among the most valuable tools available to build ecosystem and past ecosystem models. The perceptron multilayer uses the sigmoid non-

Table 1
Geographic location of sites and chronologies from Northwestern Argentina.

Site	Latitude	Longitude	Period	Species
El Arrasayal – Salta	− 22°44′	− 64°32′	1765–1985	*Juglans australis*
Río Bolsas, Piedra Parada – Jujuy	− 23°55′	− 65°19′	1689–1981	*Juglans australis*
Finca del Rey – Salta	− 24°36′	− 64°35′	1810–1981	*Cedrella angustifolia*
Río La Sala – Salta	− 24°36′	− 64°35′	1849–1981	*Juglans australis*
Río Blanco – Jujuy	− 24°55′	− 65°25′	1850–1981	*Cedrella angustifolia*
Los Laureles – Salta	− 25°07′	− 65°33′	1826–1979	*Juglans australis*
Finca Las Pichanas – Salta	− 26°05′	− 65°23′	1848–1981	*Juglans australis*
Río Horqueta – Tucumán	− 27°08′	− 65°51′	1783–1982	*Juglans australis*
Dique Escaba – Tucumán	− 27°42′	− 65°47′	1813–1985	*Juglans australis*

Table 2
Geographic location of sites and chronologies from Patagonia.

Site	Latitude	Longitude	Period	Species
La Esperanza – Río Negro	− 41°15′	− 71°54′	− 342–1995	*Fitzroya cupressoides*
Río Motoco – Chubut	− 42°05′	− 71°50′	320–1993	*Fitzroya cupressoides*
Río Cisne – Chubut	− 42°09′	− 71°33′	441–1974	*Fitzroya cupressoides*
Puerto Café – Chubut	− 42°44′	− 71°58′	311–1992	*Fitzroya cupressoides*

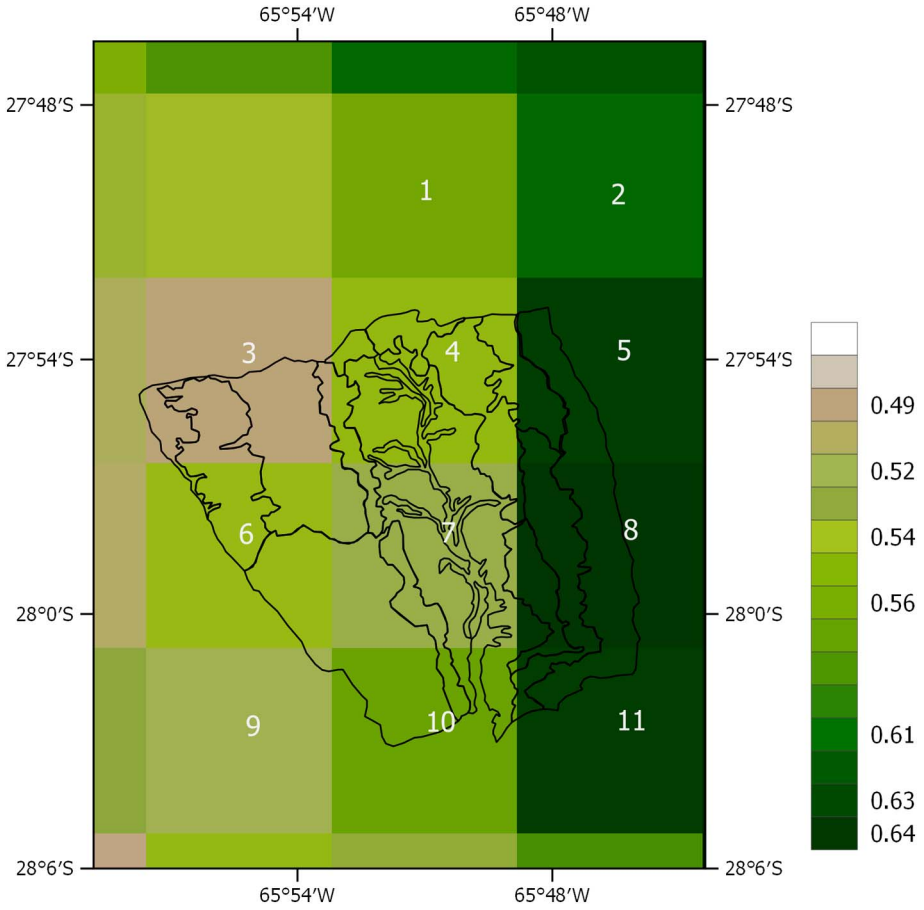

Fig. 4. NDVI annual average of north of Valle de Catamarca pixels (Catamarca, Argentina).In black the contour of vegetation units of Valle de Ambato.

linear function that is differentiable and therefore useful for the weight learning algorithm. These attributes allow the ANNs to deal with the same problems as the linear models and further extrapolate on the basis of rules learned during the training.

There are three steps to produce hindcasts: training, validation and hindcasting.

4. Results

4.1. Training

Annual tree-ring width data are entered together with annual NDVI data for the period of 1981–1998 for all three 8 km-pixels (2, 5 and 6); each pixel covers an area of 64 km^2. The vegetation units described by Cabrera (1976), Morláns (1995) and de la Orden and Quiroga (1997) were used as ground truth, to verify validity of the training results. Pixels in the Yunga describe a montane tropical forest and that of the Chaco Serrano describes a dry forest and shrub (Fig. 4).

Real values of NDVI from pixel 2 range between 0.55 and 0.67; those from pixel 5 are more stable and range between 0.61 and 0.66; pixel 6 has a high NDVI variation range, from 0.44 to 0.63. (Table 3, Fig. 4).

Table 3
Average values and NDVI range, period 1981–1998 for pixels 2, 5 and 6, north of Valle de Catamarca.

Pixel	NDVI annual average	NDVI range variation
2	0.61	0.55–0.67
5	0.63	0.61–0.66
6	0.54	0.44–0.63

4.2. Validation of training results

The ANN model training produced annual simulation data for the period of 1981–1998 for each pixel. Since the available sample collection of NDVI of satellite data for training is small (18 years), a feasible way of validation is the comparison between prediction and observation. Therefore, the validation method used was the comparison between the model output with data collected from observations. Thus, these simulated data were directly compared with the real NDVI data showing a good coincidence. Pearson correlation for data and simulations were as follows, pixel 2 (r = 0.90), pixel 5 (r = 0.89) and pixel 6 (r = 0.83) (Fig. 5).

4.3. Hindcasting

The annual NDVI hindcasts for the periods of 550–650 CE and 1550–1650 CE are shown in Figs. 6a and b, respectively. In both periods, the paleo-NDVI values were higher in pixels 2 and 5 than those in pixel 6. Paleo-NDVI of pixel 2 showed a high variation (0.40 to 0.75), while pixel 5 appeared more stable (0.58 to 0.67). On the other hand, pixel 6 showed large variations (0.30 to 0.64).

In the early period, 550–650 CE, large fluctuations are seen in pixels 2 and 6 between 600 and 615 CE with contrasting trends. In pixels 2 and 6 paleo-NDVI values diminish while pixel 5 remains stable in the same lapse.

In the late period, 1550–1650 CE, paleo-NDVI values fluctuate in all three pixels. Between 1603 and 1620 CE, paleo-NDVI values diminish in pixels 2 and 5, and increase in pixel 6.

In the early period, the paleo-NDVI anomalies sporadically show positive and negative ones in the range of 1 through 2 Standard Deviations (SD) in all three pixels. Between 597 and 615 CE, paleo-NDVI shows extreme anomalies (larger than 2 SD), negative for pixel 2

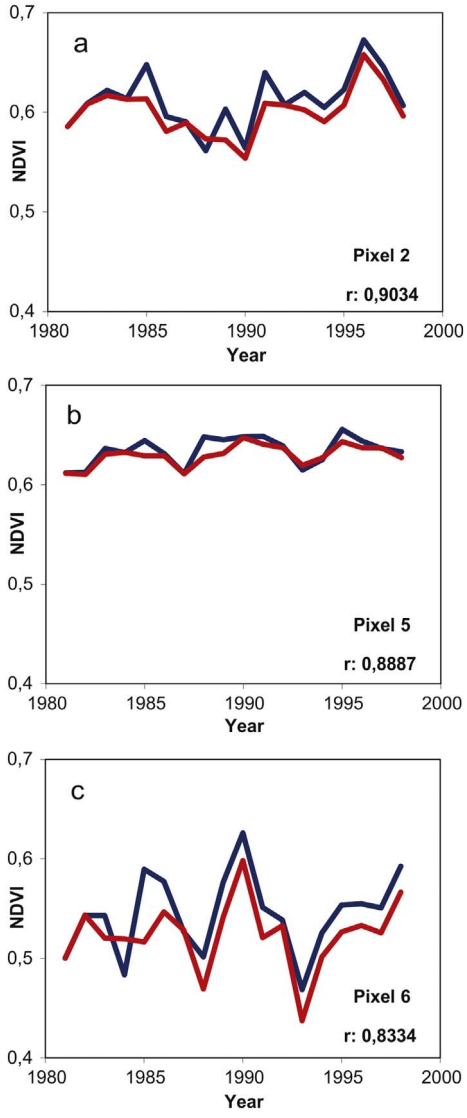

Fig. 5. NDVI annual average (blue) and predicted (red) with ANN are shown for the period of 1981–1998, a) pixel 2, b) pixel 5, c) pixel 6. Coefficient r is Pearson correlation between observed and predicted NDVI. (For interpretation of the references to colour in this figure legend, the reader is referred to the web version of this article.)

and positive for pixel 6. Meanwhile, pixel 5 only shows a few extreme positive ones (Fig. 7a).

In the late period, extreme anomalies are shown between 1604 and 1620. These are positive in pixel 6 and negative in pixel 5 (Fig. 7b). Toward the end of this period, positive anomalies are shown in pixel 2 and negative ones in pixel 5.

5. Discussion

In the modern system, the annual NDVI values of the three pixels north of Valle de Catamarca showed relevant differences. The one from the west, belonging to the driest area evidenced the lowest values (0.54) and a great interannual variability, while those from the east, more humid, showed higher values (> 0.6). Although the eastern pixels belong to the same phytogeographical province (Yunga), the differences observed in relation to the interannual variability might be due to the environmental heterogeneity in pixel 5. Here, a broad grassland belt on top of the hills and a forest at both slopes develop (FAO, 2014; de la Orden and Quiroga, 1997; Morláns, 1995) (Figs. 1 and 2).The vegetation heterogeneity would smooth the NDVI growth or decrease that could suffer the forest. In the meantime, pixel 2 presents great NDVI

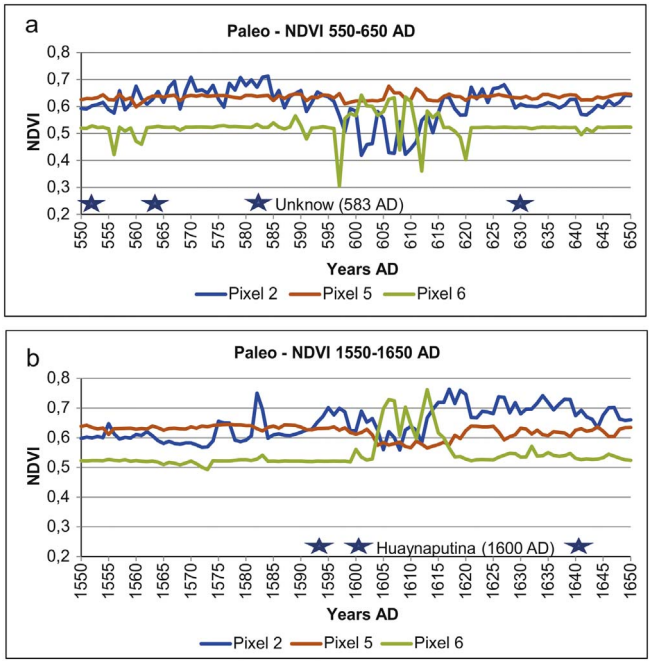

Fig. 6. Paleo-NDVI of three pixels from north of Valle de Catamarca, a) period 550–650 CE, b) period 1550–1650 CE. Volcanic eruptions.

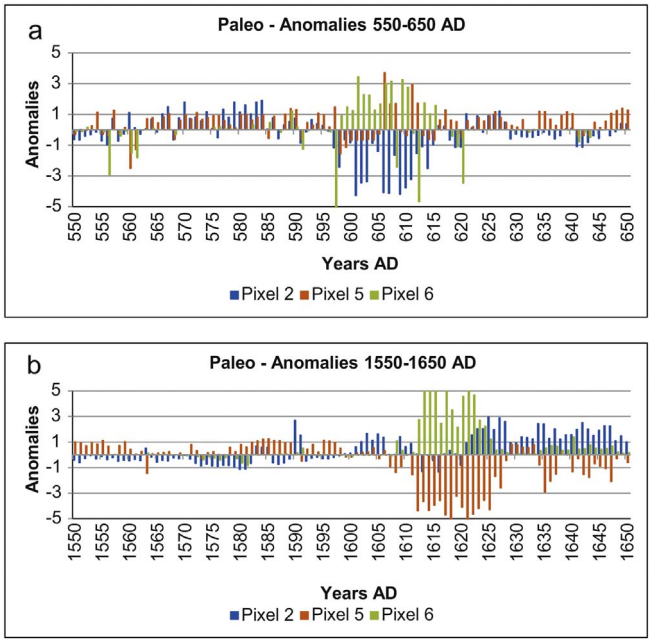

Fig. 7. NDVI paleo-anomalies of three pixels from north of Valle de Catamarca, a) period 550–650 CE, b) period 1550–1650 CE.

fluctuations because it corresponds mainly to a forest, and this vegetation type is sensitive to changes at a regional level.

This same behavior was observed in the hindcasting of the three pixels: pixel 5 was less sensitive to the climate forcings with regional reach; pixels 2 and 6 had relevant variations, although of opposite sign.

Methodologically, the ANN models for hindcasting paleo-NDVI showed the strength of the non-linear function used by these models. Our hindcasts appear well related to climate forcings as well as other factors, probably of local to regional importance.

Effects of the volcanic climate forcing were brought to light in our hindcasting. Besides their intrinsic value in the hindcasts, the volcanic data are completely independent of our research and hence provide a

source of cross-validation.

For the early period (550–650 CE), the volcanic record of Plateau Remote (Antarctica) includes four volcanic events, with maximum sulfate concentration above 200 μg/kg of ice. Specifically, the event of 583 CE lasting 6.3 years (Cole-Dai et al., 2000) may be responsible for the positive and negative extreme variations of NDVI (around 597 CE) in response to a cooler climate in the Valle de Catamarca. Rather than a lag effect, this delayed response should obey to the residence of the eruption gasses and particles in the stratosphere.

For the late period (1550–1650 CE), three eruptions of global reach brought up the sulfate concentration values to the range of 181–237 μg/kg of ice. Particularly, in 1600 CE (Cole-Dai et al., 2000) and between 1599 and 1604 CE, Budner and Cole-Dai (2003) found high concentrations of sulfuric acid associated with the activity of the Huaynaputina volcano (in the vicinity of Arequipa, Peru). The Indians, priests and viceroy chronicles (Domínguez, 2007) describing a large magnitude eruption in February of 1600, was probably the largest eruption in the historical period of South America (de Silva and Zielinski, 1998). This event is reflected in our NDVI hindcasts by the extreme (positive and negative) deviations between 1604 and 1620 years AD.

In the Yunga, Lupo et al. (2006) identified important changes in sedimentation rate in one of the Yala Lagoons (El Rodeo), together with increases of organic phosphorus and carbon. These scientists associated their observations with the impact of agriculture in the beginnings of the Spanish colony, erosion related to an increase of rainfall. At the small spatial scale they work, Lupo and collaborators confront the difficulty to tell apart the effects of human impact and global climate forcings. This is an interesting problem for future research.

A single variation in the solar irradiance received at ground level (due to the presence of volcanic particles and aerosols in the atmosphere) may produce different results in different ecosystems. Considering a humid and a dry forest, the irradiance change will affect that which is water-saturated by reduction of the photosynthetically active radiation (PAR), and the dry one by a reduction of the evapotranspiration.

The extreme anomalies in paleo-NDVI occurring in the early and late periods were associated to global cooling produced by volcanic activity. The anomalies were of opposite sign in the Yunga and Chaco Serrano ecosystems, by alteration of the respective limiting factors. In Yunga, a temperature decrease would lead to decreased rainfall (Colose et al., 2016) and hence to a decrease of paleo-NDVI values. The growth pattern of the rings of *Juglans australis* mainly reflects a direct effect of rainfall (Boninsegna et al., 2009). The relationships between temperature and precipitation in the Yunga are related to the strength of the low level jet to carry water and to the increase or decrease of warming (Boninsegna et al., 2009). The anomalies found in the dry and warm Chaco Serrano were positive. Cooling resulting from volcanic eruptions must have reduced evapotranspiration and hence increased the NDVI of xerophytic vegetation. Summing up, the contrasting behavior of NDVI in the opposite sides of the Valley is the response of different ecosystems to temperature decrease.

As regards to the accuracy of statistical information, that is, the degree to which the information correctly describes the phenomena, it was appreciated while comparing the observed with the predicted data during the model training. This validation method should be used when the available NDVI data for training are small. The hindcasting by means of ANN was also supported by the high correlation (Pearson's r) between real and hindcast data.

In closing, this dynamic hindcasting of paleo-NDVI of the different vegetation types in north Valle de Catamarca using ANN in the times of different cultures is an advance in understanding ecosystem functioning under the influence of climate forcings and cultural impacts.

6. Concluding remarks

The use of artificial neural networks (ANN) for ecosystem modeling proved to be a powerful tool to be used in archaeological studies.

Important paleo-NDVI fluctuation lasting 15 and 20 years were identified in both periods analyzed (550–650 and 1550–1650 CE).

NDVI-fluctuations identified within the period of 550–650 CE are probably related to an eruption occurred in year 583 in an unknown location but having global effects that was identified in Antarctic ice cores.

NDVI-fluctuations within the period of 1150–1650 CE have been related with eruption of the Huaynaputina volcano (SW Peru), identified in Antarctic ice cores and assigned a global influence.

The sensitivity of our model is shown by its capacity to identify changes in the paleo-NDVI. Such changes suggest a correspondence between the climatic forcing leading to a global cooling and the detected ecosystem responses in north of Valle de Catamarca.

Acknowledgements

This work was performed through grants: “Paleodietas y Paleoambientes del Holoceno de zonas áridas”, SECYT — Universidad Nacional de Mar del Plata EXA 754/16 2016-2017 and “De Climas y Paleoclimas: Materialidades, representaciones y percepciones en los Andes meridonales”, SECYT — Universidad Nacional de Córdoba. 2014–2016 UNC (Resolución Secyt 203/14 and Resolución Rectoral 1565/14) - SECyT. PIP/CONICET 112/2011 01 00548.

References

Adya, M., Collopy, F., 1998. How effective are neural networks at forecasting and prediction? A review and evaluation. J. Forecast. 17, 481–495. http://dx.doi.org/10.1002/(SICI)1099-131X(1998090)17:5/6<481::AID-FOR709>3.0.CO;2-Q.

Bandyopadhyay, G., Chattopadhyay, S., 2007. Single hidden layer artificial neural network models versus multiple linear regression model in forecasting the time series of total ozone. Int. J. Environ. Sci. Technol. 4, 141. http://dx.doi.org/10.1007/BF03325972.

Bard, E., Raisbeck, G., Yiou, F., Jouzel, J., 1997. Solar modulation of cosmogenic nuclide production over the last millennium: comparison between ^{14}C and ^{10}Be records. Earth Planet Sci. Lett. 150, 453–462. http://dx.doi.org/10.1016/S0012-821X(97)00082-4. ISSN: 0012-821X.

Bard, E., Raisbeck, G., Yiou, F., Jouzel, J., 2000. Solar irradiance during the last 1200 years based on cosmogenic nuclides. Tellus B 52 (3), 985–992. http://dx.doi.org/10.1034/j.1600-0889.2000.d01-7.x. ISSN: 0280-6509.

Bard, E., Raisbeck, G., Yiou, F., Jouzel, J., 2003. Reconstructed Solar Irradiance Data. IGBP PAGES/World Data Center for Paleoclimatology Data Contribution Series #2003-006. NOAA/NGDC Paleoclimatology Program, Boulder, CO, USA. ftp://ftp.ncdc.noaa.gov/pub/data/paleo/climate_forcing/solar_variability/bard_irradiance.txt (web archive link, 08 August 2015) (access: 08/08/2015).

Bard, E., Raisbeck, G., Yiou, F., Jouzel, J., 2007. Comment on “Solar activity during the last 1000 yr inferred from radionuclide records” by Muscheler et al. 2007. Quat. Sci. Rev. 26, 2301–2308. http://dx.doi.org/10.1016/j.quascirev.2007.06.002. ISSN: 0277-3791.

Boninsegna, J.A., Argollo, J., Aravena, J.C., Barichivich, J., Christie, D., Ferrero, M.E., Lara, A., Le Quesne, C., Luckman, B.H., Masiokas, M., Morales, M., Oliveira, J.M., Roig, F., Srur, A., Villalba, R., 2009. Dendroclimatological reconstructions in South America: a review. Palaeogeogr. Palaeoclimatol. 281, 210–228. http://dx.doi.org/10.1016/j.palaeo.2009.07.020.

Budner, D., Cole-Dai, J., 2003. The number and magnitude of large explosive volcanic eruptions between 904 and 1865 A.D.: quantitative evidence from a new South Pole ice Core. In: Robock, A., Oppenheimer, C. (Eds.), Volcanism and the Earth's Atmosphere, Geophysical Monography. 139 American Geophysical Union, Washington. http://dx.doi.org/10.1029/139GM10.

Burry, L.S., Palacio, P.I., Somoza, M., Trivi de Mandri, M.E., Lindskoug, H.B., Marconetto, M.B., D'Antoni, H.L., 2017. Dynamics of fire, precipitation, vegetation and NDVI in dry forest environments in the North-West of NW Argentina. J. Archaeol. Sci. Rep. http://dx.doi.org/10.1016/j.jasrep.2017.05.019.

Cabrera, A., 1976. Regiones fitogeográficas argentinas. In: Enciclopedia Argentina de Agricultura y Jardinería. 2. pp. 1–85.

Cigizoglu, H.K., 2003. Estimation, forecasting and extrapolation of river flows by artificial neural networks. Hydrolog. Sci. J. 48 (3), 349–361. http://dx.doi.org/10.1623/hysj.48.3.349.45288.

Cole-Dai, J., Mosley-Thompson, E., Wight, S.P., Thompson, L.G., 2000. A 4100-year record of explosive volcanism from an East Antarctica ice core. J. Geophys. Res.-Atmos. 105 (14), 24431–24441.

Colose, C.M., LeGrande, A.N., Vuille, M., 2016. The influence of volcanic eruptions on the

climate of tropical South America during the last millennium in an isotope-enabled general circulation model. Clim. Past 12, 961–979. www.clim-past.net/12/961/2016/. doi:http://dx.doi.org/10.5194/cp-12-961-2016.

Costa, F., Scaillet, B., Gourgaud, A., 2003. Massive atmospheric sulfur loading of the AD 1600 Huaynaputina eruption and implications for petrologic sulfur estimates. Geophys. Res. Lett. 30, 1068. http://dx.doi.org/10.1029/2002GL016402,2.

D'Antoni, H.L., 2008. Arqueoecología Sistémica y Caótica. In: Colección Textos Universitarios 41. CSIC, Madrid 278 p. ISBN 978-84-00-08629-9.

D'Antoni, H.L., Mlinarevic, A., 2002. Past sea surface temperature derived from tree rings. In: Astrobiology Science Conference (Presenter 28). NASA Ames Research Center, Moffet Field, California.

D'Antoni, H.L., Peterson, D.L., Mlinarevic, A., 2002. Rapid rates of change in South American vegetation linked to 'El Niño' Southern Oscillation. In: Astrobiology Science Conference (Presenter 29). NASA Ames Research Center, Moffet Field, California.

D'Antoni, H.L., Skiles, J.W., Schultz, C., Zamora, J., Mendonça, J., 2008. The Hindcasting Ecosysytem Model (HEMO), End Report to NASA Astrobiology Institute. NASA Ames Research Center, Moffet Field, California.

de la Orden, A., Quiroga, A., 1997. Fisiografía y vegetación de la Cuenca del Río Los Puestos, Departamento de Ambato, Catamarca. Rev. Cienc. Técnica 4 (4), 27–45.

de Silva, S.L., Zielinski, G.A., 1998. Global influence of the 1600 eruption of Huaynaputina, Peru. Nature 393, 455–458. http://dx.doi.org/10.1038/30948.

Domínguez, N., 2007. La erupción del Volcán Huaynaputina en el año 1600. http://laicacota.blogspot.com.ar/2007/03/huaynaputina-1600.html.

FAO, 2014. Global Land Cover (GLC-SHARE) Beta-Release 1.0 Database, Land and Water Division, John Latham, Renato Cumani, Ilaria Rosati and Mario Bloise. http://www.fao.org/uploads/media/glc-share-doc.pdf.

Hall, M., Frank, E., Holmes, G., Pfahringer, B., Reutemann, P., Witten, I.H., 2009. The WEKA data mining software: an update. SIGKDD Explor. 11 (1), 10–18. http://dx.doi.org/10.1145/1656274.1656278. ISSN: 1931-0153.

Hunzinger, H., 1997. Hydrology of montane forests in the Sierra de San Javier, Tucumán, Argentina. Mt. Res. Dev. 17 (4), 299–308. http://dx.doi.org/10.2307/3674020.

Insel, N., Poulsen, C.J., Elers, T.A., 2010. Influence of the Andes Mountains on South American moisture transport, convection, and precipitation. Clim. Dyn. 35, 1477. http://dx.doi.org/10.1007/s00382-009-0637-1.

Jiang, S., Cole-Dai, J., Li, Y., Ferris, D.G., Ma, H., An, C., Shi, G., Sun, B., 2012. A detailed 2840-year record of explosive volcanism in a shallow ice core from Dome A, East Antarctica. J. Glaciol. 58, 65–75. http://dx.doi.org/10.3189/2012JoG11J138.

Lara, A., Villalba, R., Aravena, J., Wolodarsky, A., Neira, E., 2000. Desarrollo de una red de cronologías de *Fitzroya cupressoides* para Chile y Argentina, in Roig F. (Compil.), Dendrocronología en América Latina. EDIUNC, Mendoza. pp. 217–244. http://www.ediunc.uncu.edu.ar/catalogo/ficha/83/Dendrocronologa-en-Amrica-Latina. ISBN: 950-39-0122-7.

Lavallé, B., 2011. Miedos terrenales, angustias escatológicas y pánicos en tiempos de terremotos en el Perú a comienzos del siglo XVII, e-Spania [En ligne], 12 | décembre 2011, mis en ligne le 23 novembre 2011, consulté le 11 mai 2017. http://e-spania.revues.org/20822http://dx.doi.org/10.4000/e-spania.20822.

Lupo, L., Bianchi, M.M., Araoz, E., Grau, R., Lucas, Ch., Kern, R., Camacho, M., Tanner, W., Grosjean, M., 2006. Climate and human impact during the past 2000 years as recorded in the Lagunas de Yala, Jujuy, northwestern Argentina. Quatern Int 158, 30–43. http://dx.doi.org/10.1016/j.quaint.2006.05.015.

Marconetto, M.B., Burry, L.S., Palacio, P.I., Somoza, M., Trivi, M.E., Lindskoug, H.B., D'Antoni, H.L., 2015. Aporte a los Estudios Paleoambientales del Valle de Ambato (Catamarca) a partir de la Reconstrucción del Paleo NDVI (442–1998 AD). Mundo Antes 9, 45–68. ISSN 1514-982X/ISSN en Línea 2362-325X. http://www.mundodeantes.org.ar/pdf/revista9/02-marconetto%20x%203.pdf.

Morláns, M.C., 1995. Regiones Naturales de Catamarca. Provincias Geológicas y Provincias Fitogeográficas. Rev. Ciencia Técnica 2, 1–36. http://editorial.unca.edu.ar/Publicacione%20on%20line/Ecologia/imagenes/pdf/006-fitogeografia-catamarca.pdf.

Mosley-Thompson, E., Mashiotta, T.A., Thompson, L.G., 2003. Ice core records of late Holocene volcanism: Current and future contributions from the Greenland PARCA cores. In: Robock, A., Oppenheimer, C. (Eds.), Volcanism and the Earth's Atmosphere. Geophys. Monogr. Ser. 129. AGU, Washington, D.C., pp. 153–164. http://dx.doi.org/10.1029/139GM10.

Palmieri, C. N., zCarma, M.I., Quiroga, A. 2014. Las ecorregiones presentes en Catamarca. Atlas Catamarca- Univ. Nac. de Catamarca - Fac. de Cs. Agrarias. http://www.atlas.catamarca.gob.ar/PDF/unidades%20tematicas/territorio%20y%20medio%20ambiente/eco%20regiones/Ecorregiones_presentes_Catamarca.pdf

Palmieri, C.N., Olmos, L.R., Quiroga, A., de la Orden, E., Carma, M.I., 2005. Caracterización hidroclimática de siete localidades del Departamento Ambato, Provincia de Catamarca. Argentina. Rev. CIZAS 6, 7–17. http://editorial.unca.edu.ar/Publicacione%20on%20line/CIZAS/imagenes/pdf/V6/1.palmieri.pdf.

Paruelo, J.M., Tomasel, F., 1997. Prediction of functional characteristics of ecosystems: a comparison of artificial neural networks and regression models. Ecol. Model 98 (2), 173–186. http://dx.doi.org/10.1016/S0304-3800(96)01913-8. ISSN: 0304-3800.

Russell, S., Norvig, P., 2003. Artificial Intelligence: A Modern Approach, 2nd Ed. Prentice Hall Series in Artificial Intelligence Pearson Education, Inc., Upper Saddle River, New Jersey 07458 1081 pp. ISBN 978-0136042594.

Tucker, C.J., Sellers, P., 1986. Satellite remote sensing of primary production. Int. J. Remote Sens. 7 (11), 1395–1416. http://dx.doi.org/10.1080/01431168608948944.

Tucker, C.J., Pinzon, J.E., Brown, M.E., 2004. Global Inventory Modeling and Mapping Studies (GIMMS), AVHRR 8km Normalized Difference Vegetation Index (NDVI), Bimonthly 1981–1998. Global Land Cover Facility, University of Maryland, College Park, Maryland. https://landval.gsfc.nasa.gov/pdf/GIMMS_NDVI_8km_doc.pdf.

Villalba, R., Boninsegna, J.A., Holmes, R.L., 1985. *Cedrella angustifolia* and *Junglans australis* two new tropical species useful in dendrochronology. Tree-Ring Bull. 45, 25–35. https://www.treeringsociety.org/TRBTRR/TRBTRR.htm#Vol45.

Villalba, R., Holmes, R.L., Boninsegna, J.A., 1992. Spatial patterns of climate and tree growth variations in subtropical northwestern Argentina. J. Biogeogr. 19, 631–649. http://dx.doi.org/10.2307/2845706. ISSN: 0305-0270.

Villalba, R., Boninsegna, J.A., Lara, A., Veblen, T., Roig, F., Aravena, J.C., Ripalta, A., 1996. Interdecadal climatic variations in millennial temperature reconstructions from Southern South America. In: Jones, P.D., Bradley, R., Jouzel, J. (Eds.), Climatic Variations and Forcing Mechanisms of the Last 2000 Years. NATO ASI Series Springer, Berlin Heidelberg, pp. 161–189. https://link.springer.com/chapter/10.1007/978-3-642-61113-1_9.

Virji, H., 1981. A preliminary study of summertime tropospheric circulation patterns over South America estimated from cloud winds. Mon. Weather. Rev. 109, 599–610. http://dx.doi.org/10.1175/1520-0493(1981)109<0599:APSOST>2.0.CO;2. http://journals.ametsoc.org/doi/pdf/10.1175/1520-0493%281981%29109%3C0599%3AAPSOST%3E2.0.CO%3B2 ISSN: 0027-0644.

Zerda, H.R., Tiedemann, J.L., 2010. Dinámica temporal del NDVI del bosque y pastizal natural en el Chaco seco de la provincia de Santiago del Estero, Argentina. Ambiencia Guarapuava 6, 13–24. http://revistas.unicentro.br/index.php/ambiencia/article/viewFile/971/971.

Zhou, L., Li, Y., Cole-Dai, J., Tan, D., Sun, B., Ren, J., Wei, L., Wang, H., 2006. A 780 year record of explosive volcanic eruptions from the DT263 ice core from East Antarctica. Chin. Sci. Bull. 51 (18), 2189–2197. http://dx.doi.org/10.1007/s11434-006-2164-3.

Zielinski, G.A., Mayewski, P.A., Meeker, L.D., Whitlow, S., Twickler, M.S., Morrison, M., Meese, D.A., Gow, A.J., Alley, R.B., 1994. Record of volcanism since 7000 B.C. form the GISP2 Greenland ice core and implications for the volcano-climate system. Science 26, 948–952. http://www.ncbi.nlm.nih.gov/pubmed/17830082.